Journal of Statistical Physics, Vol. 107, Nos. 1/2, April 2002 (© 2002)

Lees–Edwards Boundary Conditions for Lattice Boltzmann

Alexander J. Wagner[1] **and Ignacio Pagonabarraga**[2]

Received March 8, 2001; accepted October 10, 2001

Lees–Edwards boundary conditions (LEbc) for Molecular Dynamics simulations[1] are an extension of the well known periodic boundary conditions and allow the simulation of bulk systems in a simple shear flow. We show how the idea of LEbc can be implemented in isothermal lattice Boltzmann simulations and how LEbc can be used to overcome the problem of a maximum shear rate that is limited to less then $1/L_y$ (with L_y the transverse system size) in traditional lattice Boltzmann implementations of shear flow. The only previous Lattice Boltzmann implementation of LEbc[2] requires a specific fourth order equilibrium distribution. In this paper we show how LEbc can be implemented with the usual quadratic equilibrium distributions.

KEY WORDS: Lees–Edwards; simple shear; lattice Boltzmann; boundary conditions; bounce back; two-component fluid flow.

1. INTRODUCTION

In 1972 Lees and Edwards published a seminal paper[1] describing an extension of the periodic boundary conditions for Molecular Dynamics that allows the simulation of a bulk system in a simple shear flow. The uniform shear flow steady state reached is computationally convenient because it reduces finite size effects. If moving solid walls are instead introduced to produce a shear flow, the spatial inhomogeneities induced close to the wall limit the spatial region within the simulated system that can be used to study the bulk behavior of a system under shear. LEbc ensure that the system is spatially homogeneous, so that bulk-like behavior

[1] Department of Physics and Astronomy, University of Edinburgh, JCMB Kings Buildings, Mayfield Road, Edinburgh EH9 3JZ, United Kingdom; e-mail: awagner@ph.ed.ac.uk

[2] Departament de Física Fonamental, Universitat de Barcelona, Av. Diagonal 647, 08028-Barcelona, Spain.

0022-4715/02/0400-0521/0 © 2002 Plenum Publishing Corporation

is recovered on smaller simulated systems. For lattice Boltzmann methods there is the additional problem that the shear rate is limited by a maximum shear rate which is of order $1/L_y$ with L_y the transverse system size.[3] This is required to ensure that all fluid velocities remain small compared to unity in lattice units.[4]

The original LEbc were implemented for a system of particles, with positions (r_x, r_y, r_z) and velocities (v_x, v_y, v_z) within a box of dimension (L_x, L_y, L_z). Lees and Edwards showed that by implementing a new kind of boundary condition in a Molecular Dynamics simulation a state with a uniform shear velocity profile

$$\mathbf{u} = \dot{\gamma} y \mathbf{e}_x \tag{1}$$

(where $\mathbf{e}_x$ is the unity vector in x-direction) could be achieved. The method consists of a simple recipe that imposes periodic boundary conditions on particles leaving the simulation box in the directions perpendicular to the velocity gradient $\mathbf{e}_y$. Particles leaving the box in the $\mathbf{e}_y$ direction ($r_y > L_y$) will be reinserted with their x-velocity increased by the shear velocity $\mathbf{U} = \dot{\gamma} L_y \mathbf{e}_x$ added at a position given by their periodic image displaced by the time-dependent offset $d_x = tU_x$, t being the time elapsed from an appropriate origin of times. If the particles leave the box in the $-\mathbf{e}_y$ direction ($r_y < 0$) they reappear at the position of their periodic image displaced by $-d_x$ and have the shear velocity $\mathbf{U}$ subtracted from their x-velocity.

We can describe the boundary conditions by providing the new positions r' and velocities v' of the particles after the particles have been moved by the dynamics of the algorithm

$$r'_x = \begin{cases} (r_x + d_x) \bmod L_x & r_y \geqslant L_y \\ r_x \bmod L_x & 0 \leqslant r_y < L_y \\ (r_x - d_x) \bmod L_x & r_y < 0 \end{cases} \tag{2}$$

$$r'_y = (r_y \bmod L_y)$$

$$r'_z = (r_z \bmod L_z)$$

$$v'_x = \begin{cases} v_x + U_x & r_y \geqslant L_y \\ v_x & 0 \leqslant r_y < L_y \\ v_x - U_x & r_y < 0 \end{cases} \tag{3}$$

$$v'_y = v_y$$

$$v'_z = v_z$$

This is the best known way of implementing boundary conditions that allow the simulation of a bulk material under shear.

This method works well for all particle-based simulation methods. The aim of this paper is to adapt this method for lattice Boltzmann models, where the fundamental quantity is a distribution function, rather than a set of particles, which is defined on a unit lattice. In this case, the generalization of LEbc is not straightforward since the displacement d_x will in general not correspond to a full integer multiple of the lattice-spacing and it is not clear how to implement the required velocity shift in a method with a fixed set of velocities. In an earlier paper[2] one of the authors introduced an interpolation method to deal with the first problem and a partial Galilean transformation which was used to add momentum. This approach required the use of an extended equilibrium distribution function. Hence, it was not applicable to standard lattice-Boltzmann models.

In this paper we develop an alternative approach to impose Lees–Edwards boundary conditions in standard lattice-Boltzmann models. It is based on applying a Galilean-transformation and imposing the appropriate change of momentum across the moving plane. Additionally, we must displace the densities appropriately with an interpolation scheme. The derived method of Galilean transformations is quite general and we can re-derive the correct boundary conditions for a moving solid wall in contact with the fluid which were originally introduced by A. Ladd.[5]

After describing the lattice-Boltzmann model, we will discuss in detail the implementation of Lees–Edwards boundary conditions, and we will subsequently validate the method by examining implementations for binary fluid mixtures in two dimensions.

2. LATTICE BOLTZMANN MODEL

The lattice Boltzmann method can be viewed as a simple discretization of the Boltzmann equation where space is represented by a lattice and the one-particle distribution functions (which we will refer to as "*densities*"[3]) $f_i(\mathbf{x}, t)$ exist at each node $\mathbf{x}$ of the underlying lattice, for only a small number of velocities, $\{\mathbf{v}_i\}$, that (with unit time step) usually connect a small subset of lattice points. These densities evolve following a discrete-time dynamics. In each iteration, the densities are moved along their corresponding velocity vectors during the streaming step to the appropriate neighboring site, while in the subsequent collision step the set of densities at a given node are relaxed toward equilibrium. This relaxation step is

[3] These densities correspond to the probability density function in the continuous Boltzmann equation.

performed ensuring mass and momentum conservation at each node. The energy is usually not conserved (although energy conserving schemes also exist[6]) but it is possible to introduce a nominal temperature, that can be viewed as the effect of an underlying thermostat. This temperature is introduced as a parameter of the equilibrium distribution function (see below). The evolution of the densities in each time step can be written as

$$f_i(\mathbf{x}+\mathbf{v}_i, t+1) = f_i(\mathbf{x}, t)+\frac{1}{\tau}\left(f_i^0(\rho(\mathbf{x}, t), \mathbf{u}(\mathbf{x}, t))-f_i(\mathbf{x}, t)\right) \tag{4}$$

where τ is a relaxation parameter, which in the hydrodynamic limit of this equation is related to the viscosity of the fluid. Equation (4) can be viewed as the discretized version of BGK approximation of the Boltzmann equation. The linearized collision operator can be generalized to allow for several relaxation parameters (and hence the existence of different viscosities for the fluid).[5] In numerical applications the above evolution equation is usually split into two subroutines, a collision and a streaming step. The collision step is local

$$\hat{f}_i(\mathbf{x}, t) = f_i(\mathbf{x}, t)+\frac{1}{\tau}\left(f_i^0(\rho(\mathbf{x}, t), \mathbf{u}(\mathbf{x}, t))-f_i(\mathbf{x}, t)\right) \tag{5}$$

and the streaming step moves densities along their associated velocity vectors

$$f_i(\mathbf{x}+\mathbf{v}_i, t+1) = \hat{f}_i(x, t) \tag{6}$$

In the above equations, f_i^0 is the equilibrium distribution function that determines the thermodynamics of the fluid, while ρ and $\rho\mathbf{u}$ are the local mass and momentum densities. These are the macroscopic quantities of interest, and can be obtained from the densities f_i as appropriate moments

$$\rho = \sum_i f_i, \qquad \rho\mathbf{u} = \sum_i f_i\mathbf{v}_i \tag{7}$$

The choice of the equilibrium densities is one of the key ingredients of the model. They are chosen to recover the equilibrium density and momentum

$$\rho = \sum_i f_i^0, \qquad \rho\mathbf{u} = \sum_i f_i^0\mathbf{v}_i \tag{8}$$

and the appropriate pressure tensor in equilibrium

$$\mathscr{P}_{\alpha\beta} = \sum_i f_i^0 (v_{i\alpha} - u_\alpha)(v_{i\beta} - u_\beta) \tag{9}$$

where $\mathscr{P}$ is the sum of the thermodynamic pressure tensor P and an additional term that is required for Galilean invariance of the system:[7]

$$\mathscr{P}_{\alpha\beta} = P_{\alpha\beta} + \frac{\tau - 0.5}{3} (u_\alpha \partial_\beta \rho + u_\beta \partial_\alpha \rho) \tag{10}$$

Using the thermodynamic pressure tensor P is one of the standard ways to impose the desired thermodynamic behavior of the lattice-Boltzmann fluid.[8] In the simplest case, the pressure tensor for the ideal gas is $P_{\alpha\beta} = \rho \frac{1}{3} \delta_{\alpha\beta}$. We need an additional constraint for the third moment

$$\sum_i f_i^0 v_{i\alpha} v_{i\beta} v_{i\gamma} = \frac{\rho}{3} (u_\alpha \delta_{\beta\gamma} + u_\beta \delta_{\alpha\gamma} + u_\gamma \delta_{\alpha\beta}) \tag{11}$$

to ensure that the anisotropy of the underlying lattice does not affect the effective behavior of the model in the hydrodynamic limit. It is possible to fulfill these constraints by introducing equilibrium densities that depend quadratically on the lattice velocities, $\{\mathbf{v}_i\}$. Depending on the geometry of the lattice, there is still some freedom in the choice of the equilibrium densities.

A Taylor expansion to second order in the derivatives[4] of the zeroth and first moments in $\mathbf{v}$ of the lattice Boltzmann equation (4) gives the macroscopic equations which express mass and momentum conservation. From (4) we have

$$\sum_{n=1}^{\infty} \frac{1}{n!} (\partial_t + \mathbf{v}_i \nabla)^n f_i = \frac{1}{\tau} (f_i^0 - f_i) \tag{12}$$

and we can approximate

$$f_i = f_i^0 + \tau(\partial_t f_i^0 + v_{i\alpha} \partial_\alpha f_i^0) + O(\partial^2) \tag{13}$$

The zeroth velocity moment of (4) up to $O(\partial^2)$ gives the continuity equation

$$\partial_t \rho + \partial_\alpha (\rho u_\alpha) = 0 \tag{14}$$

and the first velocity moment gives the Navier Stokes equations (with $\partial_\alpha \mathbf{uuu} = O(\partial^3)$)

$$\rho \partial_t u_\alpha + \rho u_\beta \partial_\beta u_\alpha = -\partial_\beta P_{\alpha\beta} + \partial_\beta \left[\rho \nu \left(\partial_\beta u_\alpha + \partial_\alpha u_\beta - \frac{2}{D} \partial_\gamma u_\gamma \delta_{\alpha\beta} \right) \right] \tag{15}$$

where the viscosity is $\nu = (\tau - 0.5)/3$ and D is the number of spatial dimensions. In order to simulate a mixture of two components A and B we follow Orlandini[8] and define a second lattice Boltzmann equation

$$g_i(\mathbf{x} + \mathbf{v}_i, t+1) = g_i(x, t) + \frac{1}{\tau_\phi} [g_i^0(\rho(\mathbf{x}, t), \phi(\mathbf{x}, t), \mathbf{u}(\mathbf{x}, t)) - g_i(\mathbf{x}, t)] \tag{16}$$

where the density difference (concentration) $\phi = \rho_A - \rho_B$ is defined as

$$\phi = \sum_i g_i \tag{17}$$

and is the only additional variable conserved in the dynamics. The total density is now $\rho = \rho_A + \rho_B$ and the concentration couples back into the momentum equation, Eq. (15), via the pressure tensor $P_{\alpha\beta}$ which is now a function of both ρ and ϕ. The relaxation step for the dynamics of g_i is dependent on τ_ϕ which is related to the concentration diffusivity in the hydrodynamic limit. The equilibrium densities g_i are determined, again by imposing that the local equilibrium concentration is recovered (from Eq. (17)). The additional constraints on the g_i^0 are

$$\phi u_\alpha = \sum_i g_i^0 v_{i\alpha}, \qquad \mathscr{M}_{\alpha\beta} = \sum_i g_i^0 (v_{i\alpha} - u_\alpha)(v_{i\beta} - u_\beta) \tag{18}$$

Analogously to the pressure tensor, $\mathscr{M}$ is given by a correction term for Galilean invariance[9] and the chemical potential μ:

$$\mathscr{M}_{\alpha\beta} = \Gamma \mu \delta_{\alpha\beta} + \frac{\tau_\phi - 0.5}{3} (u_\alpha \partial_\beta \phi + u_\beta \partial_\alpha \phi) \tag{19}$$

The desired thermodynamics of the fluid is determined by μ which must be consistent with the chosen $P_{\alpha\beta}$. These two quantities are normally derived from a given free energy.[4, 8] In this way one ensures their consistency, and can fix beforehand the appropriate thermodynamic behavior of the binary

fluid model. It is enough to consider equilibrium densities g_i that depend quadratically on the velocities to impose the previous requirements.

Again, we recover the hydrodynamic limit of Eq. (16) performing a Taylor expansion to second order in spatial gradients. In this case we get a convection-diffusion equation for the concentration

$$\partial_t \phi + \partial_\alpha(\phi u_\alpha) = \partial_\alpha \left\{ (\tau_\phi - 0.5) \left[\partial_\beta(\Gamma \mu(\rho, \phi)\, \delta_{\alpha\beta}) + \frac{\phi}{\rho} \partial_\beta P_{\alpha\beta} \right] \right\} \qquad (20)$$

This model has been used extensively for the simulation of two-phase flows.[2, 4, 7, 8, 10] The following derivation of the LEbc presented in the next section is, however, even more general and can be applied to most lattice Boltzmann methods.

3. LEES EDWARDS' BOUNDARY CONDITIONS

The implementation of Lees Edwards boundary conditions for lattice Boltzmann will follow the same steps as in its original implementation: we will apply periodic boundary conditions to the distribution function in the two directions perpendicular to the velocity gradient; and in the third, we will assume that an image is moving with velocity $\mathbf{U}$ with respect to the (and $-\mathbf{U}$ on the opposite side) system. In a second step, we will have to displace the densities f_i (and g_i for the binary model), taking into account that we will have to interpolate the densities from the off-lattice positions to which they stream, onto the regular lattice. So this boundary condition will be applied after the collision and before the streaming of the densities.

Let us first focus on the velocity transformation. Since we are dealing now with a distribution function, the way to implement the velocity jump when crossing the system boundary in the velocity gradient direction will be to perform a Galilean transformation, i.e., if the distribution function in the system has momentum $\rho\mathbf{u}$, its image node will have momentum $\rho(\mathbf{u}+\mathbf{U})$ if we move in the direction of the gradient, and $\rho(\mathbf{u}-\mathbf{U})$ when we leave the system in the direction opposite to the velocity gradient. In this way, we will generate a linear velocity profile with shear rate $\dot{\gamma} = \mathbf{U}/L_y$. In order to get the momentum transfer, we need to calculate the difference between a density f_i at the system velocity and the one after the Galilean transformation has been applied. All the macroscopic variables and their derivatives will be the same, since the image system is moving as a block at constant velocity. So, using Eq. (13), where we retain only the u-dependence of the f's, we obtain

$$\begin{aligned}\Delta f_i &= f_i(\mathbf{u}+\mathbf{U}) - f_i(\mathbf{u}) \\ &\approx f_i^0(\mathbf{u}+\mathbf{U}) - f_i^0(\mathbf{u}) \\ &\quad -\tau\{\partial_t[f_i^0(\mathbf{u}+\mathbf{U}) - f_i^0(-\mathbf{u})] + v_{i\alpha}\partial_\alpha[f_i^0(\mathbf{u}+\mathbf{U}) - f_i^0(\mathbf{u})]\}\end{aligned} \tag{21}$$

where Δf_i is the change in the density moving in the i direction due to the Galilean transformation. Note that the transformation will only be applied to the densities crossing the LE boundary but not to the rest of the densities at the same node.

The terms linear in τ are of order $O(\partial)$ and their zeroth and first moments are $O(\partial^3)$. These terms are therefore small and enters only into the pressure moments. Therefore we can neglect them. We obtain for the boundary condition

$$f'_i = f_i + f_i^0(\mathbf{u}+\mathbf{U}) - f_i^0(\mathbf{u}) \tag{22}$$

where f'_i means the density after the application of the boundary condition. We now need to specify the equilibrium distribution. We will assume the usual quadratic distribution function which can fulfill the conditions (8) and (9):

$$f_i^0 = \rho a_0^i + \rho a_1^i v_{i\alpha}u_\alpha + a_2^i v_{i\alpha}v_{i\beta}\Pi_{\alpha\beta} + a_3^i \,\mathrm{tr}(\Pi) \tag{23}$$

where $\Pi_{\alpha\beta} = P^0_{\alpha\beta} + \rho u_\alpha u_\beta$ and we obtain

$$\begin{aligned}f_i^0(\mathbf{u}+\mathbf{U}) - f_i^0(\mathbf{u}) = \rho[&a_1^i v_{i\alpha}U_\alpha + a_2^i v_{i\alpha}v_{i\beta}(u_\alpha U_\beta + u_\beta U_\alpha + U_\alpha U_\beta) \\ &+ a_3^i(2\mathbf{u}.\mathbf{U} + |\mathbf{U}|^2)]\end{aligned} \tag{24}$$

If we have a binary mixture, the same transformation will apply to the densities g_i related to the concentration. The equilibrium distribution g_i^0 can be written in the same form as Eq. (23) if we replace ρ by ϕ and $P_{\alpha\beta}$ by $\Gamma\mu\delta_{\alpha\beta}$. In the previous expression Γ is a factor which, together with the relaxation parameter τ_ϕ, will determine the diffusivity of the concentration; $\delta_{\alpha\beta}$ is the Kronecker delta function.

Now that we have defined a suitable Galilean transform, we have to split the densities into an untransformed part and a transformed part that will stream over the boundary, i.e., the densities at the top and bottom boundaries with associated velocities $v_{iy} > 0$ and $v_{iy} < 0$ respectively if we take $\mathbf{e}_y$ as the direction of the shear gradient. It is important to ensure that the two subsets of velocities conserve the node density after the Galilean transformation has been applied. This requires

$$
\begin{aligned}
0 &= \sum_{v_{iy}>0} \Delta f_i \\
&= \sum_{v_{iy}>0} [f^0(\mathbf{u}+\mathbf{U}) - f^0(\mathbf{u})] \\
&= \sum_i \frac{(v_{iy}^2 + v_{iy})}{2} [f^0(\mathbf{u}+\mathbf{U}) - f^0(\mathbf{u})] \\
&= \frac{1}{2}(P_{yy} + \rho u_y u_y - P_{yy} - \rho u_y u_y)
\end{aligned} \tag{25}
$$

where $\sum_{v_{iy}>(<)0}$ is performed over the velocity directions with a positive (negative) component crossing the shear boundary. Equation (25) is fulfilled if we require that the velocity subset that characterizes the lattice Boltzmann model involves only velocities that do not span beyond the closest site layer, i.e., the factor $(v_{iy}^2 + v_{iy})/2$ is 1 for velocities with $v_y > 0$ and 0 otherwise. This is the case for most standard velocity sets and for the velocity set we will consider here [see Eq. (30)] in particular. To derive this result we have also used that the velocity-shift is parallel to the boundary, i.e., $U_y = 0$.

It is worth remembering that the total momentum in the direction of the velocity gradient in the system must be zero; otherwise there will be a net mass transfer across the LE boundaries which would result in an increase (or decrease) of momentum in the direction of the velocity gradient. The mean velocity will then steadily increase until it exceeds the maximum velocity and the simulation becomes numerically unstable. This is a general requirement of any Lees–Edwards boundary condition, because the presence of LE boundaries breaks the momentum conservation unless the mass transfer is exactly balanced in both directions.

The idea of the Galilean transformation that we have derived also has more general applications and can be used to derive the boundary conditions for a solid moving wall. At a solid wall, the velocity of the fluid must be that of the wall. This no-slip boundary condition for a stationary wall is implemented through the "bounce-back" method.[11] In it, one replaces the streaming step of Eq. (6) for the densities that would have been streamed through the wall with

$$f_i(\mathbf{x}, t+1) = f_{-i}(\mathbf{x}, t) \tag{26}$$

where $v_{-i} = -v_i$. To generalize this bounce back mechanism for a moving wall we first perform a Galilean transformation of the densities into a reference frame in which the wall is at rest. We then perform the bounce back

and then transform the densities back with an inverse Galilean transformation. We then obtain for the bounce back off a wall moving with velocity U

$$f_i(\mathbf{x}, t+1) = f_{-i}(\mathbf{x}, t) + 2\rho a_1^2 v_{i\alpha} U_\alpha \tag{27}$$

which is a result first derived with a different method by Ladd [6, Eq. (3.3)]. For this particular case, the change in the distribution function is linear in the velocity jump, rather than quadratic, as in the general case [cf. Eq. (24)].[4]

To complete the implementation of Lees–Edwards boundary conditions we also need to move the densities by the displacement of the image system, $d_x = tU_x$, which is not going to be an integer in general. We must then split the displacement in an integer part d_x^I and a real part d_x^R with $0 \leqslant d_x^R < 1$. We then shift the densities that will stream over the boundary with $v_{iy} > 0$ and $v_{iy} < 0$ respectively by

$$f'(\mathbf{x}^{\pm}, t) = (1 - d_x^R)\, f(\mathbf{x} + d_x^I, t) + d_x^R f(\mathbf{x} + d_x^I \pm 1, t) \tag{28}$$

where $x^{\pm}$ are the positions of the lattice points directly below or above the LE boundary and this shift and interpolation is applied to densities f_i with $v_{iy} = \pm 1$. That is, we have performed a linear partitioning of the moving density between the two corresponding nearest nodes. If necessary, it might be possible to improve upon this linear interpolation along the lines of ref. 13. This simple choice, however, already gives very accurate results.

While this implementation of Lees Edwards boundary conditions may seem straightforward it is not equivalent to the physical intuition. When we look at the momentum that is transfered to the transformed densities we see that

$$\begin{aligned} \sum_{v_{iy}>0} \Delta f_i v_{i\alpha} &= \sum_{v_{iy}>0} [f^0(\mathbf{u}+\mathbf{U}) - f^0(\mathbf{u})]\, v_{i\alpha} \\ &= \sum_i \frac{(v_{iy}^2 + v_{iy})}{2} v_{i\alpha} [f^0(\mathbf{u}+\mathbf{U}) - f^0(\mathbf{u})] \\ &= \frac{1}{3} \rho U_x \delta_{\alpha x} \end{aligned} \tag{29}$$

[4] According to the discussion of the previous paragraph, the density at both sides of the boundary is not modified by the bounce in the case of a moving parallel solid wall that slides along one of the boundaries of the system. For more general situations, this is not the case. For example, in the case of a moving rigid object embedded in the fluid, its velocity is not parallel to the boundary. In this case, the density inside the rigid object will be modified as a function of time. However, the presence of a rigid interface separating the inner from the outer motion of the fluid makes it possible to correct for these deviations.[12]

where we used Eq. (11) to evaluate the third moment of the velocity. The mass of the three densities $\sum_{v_{iy}>0} f_i$, is not fixed at $1/3\rho$ but depends on u_y as is easily seen. That means that the momentum that is acquired is different from the momentum that particles in a Molecular Dynamics simulation would acquire. This contradiction with physical intuition led Wagner & Yeomans[2] to propose a different lattice Boltzmann scheme where this break with intuition is avoided. They achieved this, but they had to replace the quadratic equilibrium distribution (23) with a distribution that contains terms quartic in the velocities and quadratic in the pressure tensor. In the next section we show that although the physical intuition for a Lees Edwards scheme seems to contradict our implementation it does in fact give the correct results.

4. NUMERICAL IMPLEMENTATION

We implemented a lattice with dimensions L_x, L_y and the boundaries of the simulation lattice have periodic boundary conditions. We implemented a D2Q9 model, a two dimensional model with velocities

$$\mathbf{v}_i = \left\{ \begin{pmatrix} 0 \\ 0 \end{pmatrix}, \begin{pmatrix} 1 \\ 0 \end{pmatrix}, \begin{pmatrix} -1 \\ 0 \end{pmatrix}, \begin{pmatrix} 0 \\ 1 \end{pmatrix}, \begin{pmatrix} 0 \\ -1 \end{pmatrix}, \begin{pmatrix} 1 \\ 1 \end{pmatrix}, \begin{pmatrix} -1 \\ 1 \end{pmatrix}, \begin{pmatrix} -1 \\ -1 \end{pmatrix}, \begin{pmatrix} 1 \\ -1 \end{pmatrix} \right\} \tag{30}$$

and with the coefficients given by Table I.

4.1. Multiple LE Planes

One of the limitations of Lattice-Boltzmann models to study fluids under shear arises because the maximum velocity cannot be larger than one lattice spacing per time step (and in practice must be $\lesssim 0.1$). This gives an

Table I. The Coefficients for the D2Q9 Model. There Are Two Free Parameters that We Set to $k = l = 1$ for Convenience

	a_0^i	a_1^i	a_2^i	a_3^i
$i=0$	$1-\frac{4}{3}(1-k)$	0	0	$-\frac{l+1}{l+2}$
$i=1,\ldots,4$	$\frac{2}{3}(1-k)$	$\frac{1}{3}$	$\frac{1}{2}$	$-\frac{1}{2}\frac{1}{l+2}$
$i=5,\ldots,8$	$-\frac{1}{3}(1-k)$	$\frac{1}{12}$	$\frac{1}{8}$	$-\frac{1}{8}\frac{l}{l+2}$

upper bound of order $1/L_y$ for the shear rates that can be reached with the method described so far (one cannot simply increase the lattice size while keeping the shear rate constant). This suggests that large systems with Lees–Edwards boundary conditions should be restricted to small shear-rates. We can now overcome this limitation using the present method by introducing a larger number of Lees–Edwards shear planes as one increases the L_y dimension of the simulation. We will still require, of course, that the velocity in each of the sub-lattices separated by the LEbc are no larger than about 0.1.

We will allow for N^{LE} Lees–Edwards shear planes at almost equidistant positions

$$y = Y^k = [(k-1/2)\, L_y/N^{LE}]_I \qquad \text{for} \quad k = \{1,\ldots, N^{LE}\} \tag{31}$$

where $[x]_I$ is the largest integer smaller than x. The system is then effectively cut into $N^{LE}-1$ sub-lattices that will move relative to each other with the associated jump-velocities U^k. The average shear rate for the system is therefore

$$\dot{\gamma} = \frac{\sum_{k=1}^{N^{LE}} U_k}{L_y} \tag{32}$$

and the stationary solution due to this set of LE shear planes is a linear shear profile of the form

$$\mathbf{u} = \begin{pmatrix} \dot{\gamma}(y - y_0^k) \\ 0 \\ 0 \end{pmatrix} \tag{33}$$

where y_0^k is the position of zero velocity for each sub-lattice.

At this point it may appear that the introduction of the shear-planes does introduce a local velocity profile and biases the flow but, in the absence of errors, only the global shear rate $\dot{\gamma}$, defined in Eq. (32) matters to the flow. This is easily seen if one considers a Molecular Dynamics simulation where the introduction of several shear planes is equivalent to describing the different sublattices in different frames of references, with no effect on the real dynamics. Because of this there is, of course, no merit in introducing more than one LE-plane (which establishes $\dot{\gamma}$) in Molecular Dynamics simulations. The only limit for the use of many LE-planes in lattice Boltzmann lies in the errors induced by the additional internal boundary condition and we discuss them in the following sections.

4.2. Transient Start of Shear and Stationary Profile

As a first test for the new boundary conditions we will examine the accuracy with which the algorithm simulates the start-up of a shear in a single component fluid. We consider a system with one LEbc and the initial velocity is zero. This corresponds to a system in which there is a periodic stack of slabs of fluid of width L_y each of which moves with a different velocity. The velocity of the nth slab is given by $u_x = nU$. The system will then exhibit viscous friction and the profile will converge toward a linear shear-profile. The density and pressure in this system remain constant and the velocity only has an x-component and its value only changes in the y-direction. The Navier–Stokes equation for this system gives

$$\partial_t u_x = \partial_y^2 u_x \tag{34}$$

i.e., a simple diffusion equation for the momentum. The solution for this equation for $L_y = \infty$ is well know [14, Section 52] and given by

$$u_x(y, t) = \operatorname{erf}\left(\frac{y}{2\sqrt{\nu t}}\right) \tag{35}$$

where

$$\operatorname{erf}(x) = \frac{2}{\sqrt{\pi}} \int_0^x e^{\xi^2}\, d\xi \tag{36}$$

Obtaining the solution for finite L_y is simply a linear superposition

$$u_x(y, t) = \sum_{k=-\infty}^{\infty} \frac{k}{|k|}\left[1 - \operatorname{erf}\left(\frac{y + kL_y}{2\sqrt{\nu t}}\right)\right] \tag{37}$$

which can be conveniently evaluated numerically. The agreement between the theoretical prediction and the measured velocity is very good as can be seen in Fig. 1. The error shown in the inset of Fig. 1 is largest for the early time simulations but is always below 1% of the maximum velocity.

4.3. Shear in a Two-Component Model

The previous simulation was effectively a one-component simulation and it did not test the effectiveness of the interpolation scheme given by Eq. (28). Unfortunately, it is not easy to find two-component flows under shear for which analytical solutions are known. There is, however, a method to test the errors introduced by the LEbc for a two-component

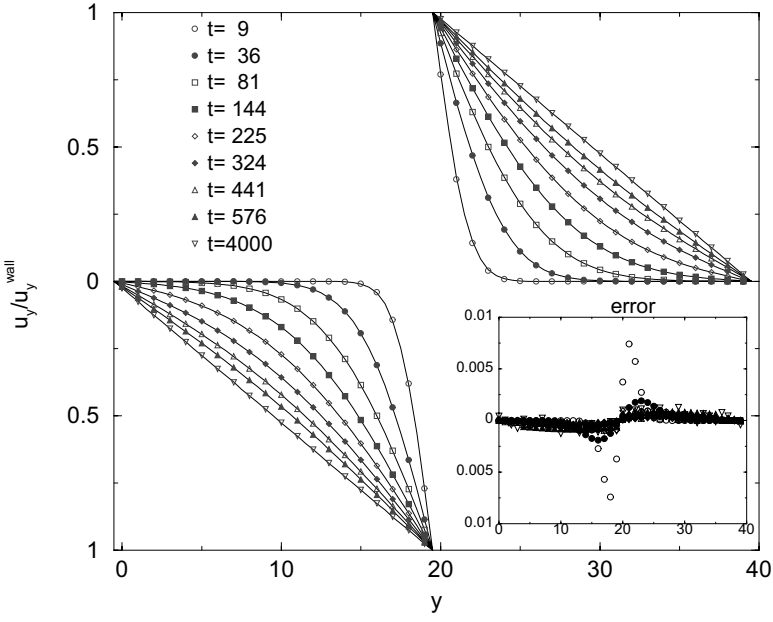

Fig. 1. Start-up of a shear profile. Solid lines are given by Eq. (37) and the symbols represent simulation data. The inset shows the difference of the theoretical and simulated velocities.

system very accurately. We can choose to have two equidistant LEbc with equal but opposite velocities so that the effective shear-rate is zero. The resulting system is then equivalent to a system at rest. We will consider two periodic stripes of A-rich and B-rich material at rest and simulate it with two LEbc with opposite velocities.

In Fig. 2 we show the results of a simulation on a 40×60 lattice with a stripe that was 20 lattice spacings wide. There were two LEbc with velocities of 0.005 and -0.005. The figure shows a section of 20×20 after 20000 iterations ($d_x = 0$) where the stripe interface overlaps the LE boundary. The full system, of course, comprises two interfaces in the x-direction and two LEbc in the y-direction and there the same error-patterns appear by symmetry.

Without errors this system would show perfectly straight contour lines and velocities of 0.005 in the upper half of Fig. 2a and -0.005 in the lower half. Since the velocities are very nearly that, we have to examine the difference of the real velocity and the predicted velocity shown in Fig. 2b. We see that this error corresponds to a deviatoric velocity profile that flows into the interface at the LEbc. We attribute this error to the fact that we use the linear interpolation from Eq. (28). The effect of this interpolation is

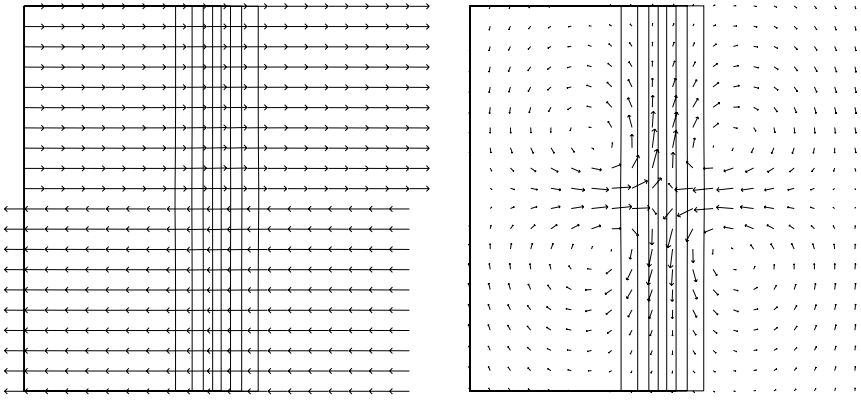

Fig. 2. A 20 by 20 section of the steady state profile of the stripe morphology. In (a) the real velocities are shown and the maximum velocity corresponds to 0.0051. In (b) the deviation from the theoretical profile is shown and the maximum velocity here is 0.00013. Eight contour lines are also shown indicating the width of the interface. (See text for details).

to smear out the interface and make it wider than the equilibrium profile. There will then be a Marangoni flow that tries to relax the profile to its equilibrium shape which we assume is the major contribution to this velocity profile. A close examination of the interface reveals a slight widening around the LEbc. The maximum amplitude of the error in the velocity is 3%. In future work we plan to examine if we can reduce this error by using an interpolation method that will conserve not only the mass but also the derivatives and prevents the additional diffusion introduced by the LEbc. Nonetheless, the accuracy found above is comparable to other sources of error (e.g., anisotropy) present in lattice Boltzmann as currently used.

As a final benchmark of the performance of LEbc's, we have studied the shape of a drop in a uniform shear flow generated by a single LE plane. In order to check for artifacts induced by the presence of the boundary, we have compared a simulation where the drop does not cross the boundary, and a situation where the LE plane bisects the drop. In Fig. 3 we show the comparison for two different capillary numbers Ca-defined as the ratio between viscous and interfacial forces, $\mathrm{Ca} = \nu R\dot{\gamma}/\sigma$, with R the radius of the drop and σ its surface tension. The interface is located in the simulation through an interpolation of the corresponding nearby nodes where the order parameter changes sign, which introduces a small source of error. The drop that is bisected by the boundary will have a larger averaged velocity. Since we are comparing the drop shapes at equal time, we have

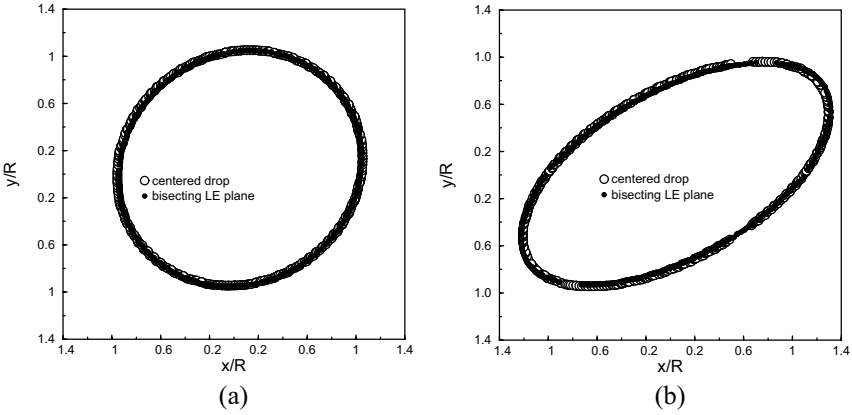

Fig. 3. Steady shapes of a drop in a Couette flow for different capillary numbers. In the open circle situation the drop does not intersect the LE plane. The filled symbols correspond to the simulation where the LE plane bisects the drop. (a) $Ca = 0.012$, (b) $Ca = 0.5$. The interfacial width in both cases is of the order of 3 in lattice units. The difference in the eccentricity of the drops, defined as the ratio of the major and minor axis, are 0.5% and 2%, respectively.

displaced the drop accordingly to make them overlay. In the figure one can clearly see that the intersection of the boundary does not affect the shape of the drop, within the numerical accuracy already mentioned in the previous paragraph.

5. CONCLUSIONS

In this paper we have described how to implement Lees–Edwards periodic boundary conditions for lattice-Boltzmann models. Lees–Edwards boundary conditions are a useful for the simulation of bulk systems under shear without the complicating influence of walls. In this way, finite size effects are diminished, which has converted the uniform shear flow in an attractive steady configuration to analyze computationally.

The implementation we have described follows the basic steps of the original paper,[1] and is compatible with the standard LB models, that assume an equilibrium distribution for the densities which is quadratic in the velocity. The numerical examples described show that the method is quantitatively accurate for single and even for two component systems.

We have also described how to avoid the limitations on the attainable shear rates that are imposed by the underlying lattice. By adding a number of shearing planes, steady states of large shear rates can then be reached (subject only to the intrinsic stability limitations of any lattice-Boltzmann

schemes). Because of the errors introduced by the interpolation scheme, it is not advisable to introduce more LEbc's than necessary. One could think of a system where the whole lattice is subject to LEbc but this would now lead to a non-isotropic diffusion. We are planing to improve the interpolation scheme in order to reduce the artificial diffusion.

ACKNOWLEDGMENTS

We thank M. E. Cates for his critical reading of this manuscript. The work was funded in part under EPSRC Grant GR/M56234 and EC Access to Research Infrastructure Contract HPRI-1999-CT-00026 TRACS program at EPCC.

REFERENCES

1. A. W. Lees and S. F. Edwards, *J. Phys. C* **5**:1921 (1972).
2. A. J. Wagner and J. M. Yeomans, *Phys. Rev. E* **59**:4366 (1999).
3. This does not apply to some new lattice Boltzmann simulations where the mean velocity is unlimited. See ref. 13.
4. A. J. Wagner, D. Phil. thesis (University of Oxford, 1997).
5. A. J. C. Ladd, *J. Fluid Mech.* **271**:285 (1994).
6. C. Teixeira, H. D. Chen, and D. M. Freed, *Comp. Phys. Comm.* **129**:207 (2000).
7. D. J. Holdych, D. Rovas, J. G. Georgiadis, and R. O. Buckius, *Internat. J. Modern Phys. C* **9**:1393 (1998).
8. E. Orlandini, M. R. Swift, and J. M. Yeomans, *Eur. Phys. Lett.* **32**:463 (1995).
9. A. J. Wagner, *in preparation*.
10. K. Langaas, D. Phil. thesis (University of Bergen, 1999).
11. U. Frisch, D. d'Humières, B. Hasslacher, P. Lallemand, Y. Pomeau, and J.-P. Rivet, *Complex Systems* **1**:649 (1987).
12. M. W. Heemels, M. H. J. Hagen, and C. P. Lowe, *J. Comput. Phys.* **164**:48 (2000).
13. C. Sun, *Phys. Rev. E* **61**:2654 (2000).
14. L. D. Landau and E. M. Lifshitz, *Fluid Mechanics*, 2nd edn. (Pergamon Press, 1993).